Establishment of a CPER reverse genetics system for Powassan virus defines attenuating NS1 glycosylation sites and an infectious NS1-GFP11 reporter virus

Jonas N. Conde,[1,2] Grace E. Himmler,[1,2,3] Megan C. Mladinich,[1,2] Yin Xiang Setoh,[4] Alberto A. Amarilla,[2] William R. Schutt,[1,5] Nicholas Saladino,[1] Elena E. Gorbunova,[1,5] Daniel J. Salamango,[1] Jorge Benach,[1,5] Hwan Keun Kim,[1,3,5] Erich R. Mackow[1,3,5]

AUTHOR AFFILIATIONS See affiliation list on p. 15.

ABSTRACT Powassan virus (POWV) is an emerging tick-borne Flavivirus that causes lethal encephalitis and long-term neurologic damage. Currently, there are no POWV therapeutics, licensed vaccines, or reverse genetics systems for producing infectious POWVs from recombinant DNA. Using a circular polymerase extension reaction (CPER), we generated recombinant LI9 (recLI9) POWVs with attenuating NS1 protein mutations and a recLI9-split-eGFP reporter virus. NS1 proteins are highly conserved glycoproteins that regulate replication, spread, and neurovirulence. POWV NS1 contains three putative N-linked glycosylation sites that we modified individually in infectious recLI9 mutants (N85Q, N208Q, and N224Q). NS1 glycosylation site mutations reduced replication kinetics and were attenuated, with 1–2 log decreases in titer. Severely attenuated recLI9-N224Q exhibited a 2- to 3-day delay in focal cell-to-cell spread and reduced NS1 secretion but was lethal when intracranially inoculated into suckling mice. However, footpad inoculation of recLI9-N224Q resulted in the survival of 80% of mice and demonstrated that NS1-N224Q mutations reduce POWV neuroinvasion *in vivo*. To monitor NS1 trafficking, we CPER fused a split GFP11-tag to the NS1 C-terminus and generated an infectious reporter virus, recLI9-NS1-GFP11. Cells infected with recLI9-NS1-GFP11 revealed NS1 trafficking in live cells and the novel formation of large NS1-lined intracellular vesicles. An infectious recLI9-NS1-GFP11 reporter virus permits real-time analysis of NS1 functions in POWV replication, assembly, and secretion and provides a platform for evaluating antiviral compounds. Collectively, our robust POWV reverse genetics system permits analysis of viral spread and neurovirulence determinants *in vitro* and *in vivo* and enables the rational genetic design of live attenuated POWV vaccines.

IMPORTANCE Our findings newly establish a mechanism for genetically modifying Powassan viruses (POWVs), systematically defining pathogenic determinants and rationally designing live attenuated POWV vaccines. This initial study demonstrates that mutating POWV NS1 glycosylation sites attenuates POWV spread and neurovirulence *in vitro* and *in vivo*. Our findings validate a robust circular polymerase extension reaction approach as a mechanism for developing, and evaluating, attenuated genetically modified POWVs. We further designed an infectious GFP-tagged reporter POWV that permits us to monitor secretory trafficking of POWV in live cells, which can be applied to screen potential POWV replication inhibitors. This robust system for modifying POWVs provides the ability to define attenuating POWV mutations and create genetically attenuated recPOWV vaccines.

KEYWORDS Powassan virus, flavivirus, reverse genetics, circular polymerase extension reaction, attenuation, NS1 glycosylation mutants, split-GFP, cell-to-cell spread

Flaviviruses (FVs) are enveloped, positive-strand RNA viruses that are globally distributed and primarily transmitted by arthropod vectors (mosquitoes and ticks) and infect an estimated 400 million people annually (1, 2). Mosquito-borne FVs cause an array of symptoms ranging from mild fevers, rashes, and jaundice to acute hemorrhagic fever, shock, microcephaly, and encephalitic syndromes (2). While FVs are widely distributed by mosquito vectors, tick-borne FVs are spread in discrete geographic locations and constrained by the range of tick vectors and their sustaining mammalian hosts (1). Tick-borne FVs cause encephalitic human diseases, with tick-borne encephalitis virus (TBEV) responsible for an estimated 10–15,000 encephalitis cases per year in Eurasia. Powassan virus (POWV) is the only tick-borne FV in North America (1) and is emerging as a cause of encephalitis in the United States (1–3). Currently, there are no approved vaccines or therapeutics for preventing or resolving POWV neurovirulence, and live attenuated recombinant POWV vaccines have yet to be developed (1, 2).

POWV is a neurovirulent tick-borne flavivirus present in tick saliva and is transmitted by injection into tick bite sites in as little as 15 min (1, 4). In symptomatic patients, POWV causes severe encephalitis with a 10% mortality rate, and 50% of cases have debilitating long-term neurologic damage (1). POWV, strain LB, was initially isolated from the brain of a 5-year old in Powassan, Ontario, Canada, in 1958 (5–7), and since then, POWVs have been found widely in *Ixodes* ticks (3, 6, 8–17). Two POWV genetic lineages are spread by discrete *Ixodes* ticks but comprise a single POWV serotype with 96% identical envelope proteins providing common vaccination targets (1, 2, 14, 15, 17). Determinants of POWV spread and neurovirulence remain to be determined but are constrained by the lack of POWV isolates derived directly from ticks, without passage in murine brains, and reverse genetics approaches for generating and comparing infectious recombinant POWV mutants.

The emergence of POWV disease parallels the spread of tick vectors in North America (2, 3, 8, 13, 18), and recent analysis revealed ~2% POWV prevalence in Long Island, NY, deer ticks (19). POWV strain LI9 was isolated from Long Island deer ticks by directly infecting VeroE6 cells, without murine neuroadaptation (5, 6, 14, 20). In epithelial cells, POWV LI9 nonlytically spreads cell-to-cell forming infected cell foci, and in mice, LI9 is neurovirulent and elicits cross-reactive neutralizing POWV antibody responses (20). How POWV spreads to neuronal compartments remains to be revealed, but the ability of POWVs to hemagglutinate (6) provides a conduit for hematogenous dissemination. *In vitro*, POWVs infect primary human brain microvascular endothelial cells (hBMECs) and, without permeabilizing polarized monolayers, POWVs are basolaterally released from hBMECs (20). Basolateral release from hBMECs provides a potential mechanism for POWVs to spread across the blood-brain-barrier into protected neuronal compartments.

Flavivirus RNAs (~11 kb) encode a single open reading frame that is cotranslationally processed by viral and cellular proteases into three structural proteins (Capsid, prM, and Envelope) and seven nonstructural (NS) proteins (2, 21, 22). FVs replicate in the cytoplasm, bud into the lumen of the ER, and are released from cells in exocytic vesicles. Envelope (Env) and NS1 proteins are both translocated into the lumen of the ER, yet only integral membrane glycoprotein Env is assembled onto the virion (23–25). Env proteins direct cellular attachment and viral entry and are the primary targets of protective neutralizing antibodies (2, 22, 26–29). In contrast to Env, translocated NS1 is glycosylated and secreted from cells and required for cytoplasmic FV replication (23, 24, 30–39). Both Env and NS1 proteins contain conserved and FV-specific glycosylation sites, and changes in the glycosylation of either protein can impact FV virulence (23–25).

NS1 is translocated into the ER lumen where it is glycosylated, dimerizes, and is secreted from cells as a lipophilic hexameric complex (30, 31, 40, 41). Within the ER, NS1 peripherally associates with, and remodels, lumenal ER membranes and nucleates the assembly of cytoplasmic FV polymerase complexes through interactions with integral membrane NS2A/4A/4B proteins (31, 32, 34, 41–43). NS1 conservation across FV groups reflects multifunctional roles for NS1 domains in ER membrane curvature, viral replication, NS1 secretion, dimer and hexamer assembly, lipid binding, and many suggested

pathogenic functions: binding complement, cell permeability, and viremia (23, 24, 31, 32, 34, 36, 38, 39, 42–45). The array of proposed NS1 functions highlights the importance of NS1 in pathogenesis and rationalizes mutating NS1 as a mechanism of FV and POWV attenuation (23–25, 42, 46–48).

Analysis of Japanese encephalitis virus (JEV) NS1 mutants distinguished NS1 residues required for replication (AA160) from viral particle formation (AA273) (38). However, mutating specific NS1 N-linked glycosylation sites (NxS/T) has been reported to either enhance or inhibit the replication and neurovirulence of discrete FVs (37, 46, 47, 49). All FV NS1 proteins have an N-linked glycosylation site at residue 207/208 (23, 25, 30, 37, 40, 50); however, POWV NS1 proteins also contain two novel glycosylation sites (N85 and N224) (23). Functions of unique POWV NS1 glycosylation sites have yet to be evaluated but may play key roles in POWV replication, secretion, cell-to-cell spread, and pathogenesis.

Reverse genetics systems are needed to genetically modify POWVs, define determinants of POWV pathogenesis, and create live attenuated recombinant POWV vaccines. Typical reverse genetics approaches are based on cloning viral RNA genomes into bacterial plasmids or artificial chromosome vectors with the toxicity and stability issues of large viral inserts that magnify the complexity of genetic virus modification (51–57). The circular polymerase extension reaction (CPER) was originally devised to clone complex genes (58, 59) and subsequently used to bypass the plasmid instability of large viral inserts and to rapidly generate mutant and reporter viruses (38, 60–65). CPER has now been used to investigate virulence determinants in West Nile virus (WNV), Zika virus, yellow fever and dengue virus (DENV), and JEV (38, 60–64, 66, 67) and has the potential to be applied to other positive-stranded RNA viruses (62, 68).

Here, we used CPER to develop a robust POWV reverse genetics system and generate an infectious LI9 POWV from cDNA (recLI9) that mirrors wild-type (WT) LI9 in sequence, replication, and focal cell-to-cell spread in VeroE6 cells. CPER was used to generate recLI9 mutant viruses lacking individual NS1 glycosylation sites (N85Q, N208Q, and N224Q). Mutating LI9 NS1 glycosylation sites reduced replication kinetics, viral titers and delayed focal cell-to-cell spread *in vitro*. The recLI9-NS1-N224Q mutant was severely attenuated with foci formation delayed by 2–3 days *in vitro* and *in vivo* resulting in the survival of 80% of peripherally inoculated mice. Our findings define a key role for the NS1-N224 glycosylation site in POWV replication, cell-to-cell spread, and pathogenesis and suggest N224Q as an attenuating mutation to be considered in the development of live attenuated POWV vaccines. In order to monitor NS1 functions, we used CPER to add a split-GFP tag to the NS1 C-terminus and generate an infectious, GFP expressing, recLI9 reporter virus (69–73). Infecting cells expressing ER-GFP$_{1-10}$ cells with the POWV GFP11 reporter virus (recLI9-NS1-GFP11) reconstituted GFP fluorescence that permits live cell analysis of NS1 spread during infection and a fluorescence-based assay for screening potential inhibitors of POWV replication and maturation (69, 70, 72, 73). The novel accumulation of NS1-GFP in large intracellular vesicles suggests a potential mechanism for POWV NS1 to regulate viral release and cell-to-cell spread (69, 74). Collectively, our robust POWV reverse genetics system permits us to define determinants of POWV pathogenesis, evaluate attenuating POWV mutations, and create genetically modified recPOWVs for use as live attenuated vaccines.

RESULTS

POWV spreads cell-to-cell in the presence of neutralizing antibody

The direct isolation of POWV LI9 in VeroE6 cells revealed a novel focal spread phenotype that occurred in the absence of restrictive overlays and without lytic plaque formation (20). POWVs bud into the lumen of the ER and are trafficked via secretory vesicles to the cell surface where they remain largely cell associated (6, 7). Foci formation suggested the potential for POWV to spread cell-to-cell similar to hepatitis C virus (HCV), a distant FV family member, that spreads focally cell-to-cell in a neutralizing antibody-independent manner (75–77). To investigate whether LI9 foci are formed by cell-to-cell spread, we

evaluated foci formation in the presence of POWV neutralizing antibody (ATCC-HMAF) or control antibody added daily to infected cell supernatants. Anti-POWV antibody added to cells during viral adsorption prevented infection, while the post-adsorption addition of control or anti-POWV antibody at a 1:250 dilution (neutralizing titer 1:6,400) failed to inhibit the formation of POWV-infected cell foci (Fig. 1A). This establishes that POWV LI9 initially spreads cell-to-cell and explains the focal spread of LI9 during isolation from ticks and during passage in epithelial cells in liquid culture. These are novel findings for tick-borne FVs that may permit POWV to bypass immune surveillance (78) and provide potential mechanisms for POWVs to spread at tick bite sites or into the CNS.

CPER reverse genetics: a mechanism for defining determinants of POWV pathogenesis

Currently, there are no established mechanisms for attenuating POWVs or defining determinants of POWV neurovirulence. To generate recombinant POWVs, we used a CPER approach (38, 60–65) to develop a robust POWV reverse genetics system (Fig. 1B through D). POWV LI9 RNA was initially used to generate first-strand cDNA that was amplified into five fragments comprising the full-length POWV genome and a sixth circularizing UTR-linker fragment (Fig. 1B). Amplified fragments contain 26 nucleotide overlapping sequences, with the UTR-linker fragment containing 26 nt from the LI9 3′UTR, a HDVr, SV40 polyadenylation signal, CMV promoter, and the first 33 nt of the 5′UTR sequence (Fig. 1C). To generate circularized CPER DNAs, LI9 F1-F5 cDNA fragments and the UTR-linker DNA were amplified using high-fidelity Phusion DNA polymerase (Fig. 1D). CPER-amplified DNA was purified and directly transfected into HEK293T or VeroE6 cells. Three days post-transfection, supernatants from transfected cells were inoculated into VeroE6 cells, and infectious viral rescue was evaluated by immunoperoxidase staining of LI9 infected cells (Fig. 1E and F). Cells infected by recLI9 retained a focal cell-to-cell spread phenotype, replication kinetics, and titers, with complete recLI9 sequences identical to WT LI9 (Fig. 1G). This demonstrates the authenticity of the CPER-generated recLI9 POWV and the development of a robust reverse genetic system for generating POWVs from recombinant DNA.

CPER mutagenesis of specific NS1 glycosylation sites inhibits POWV spread and replication

NS1 is translocated into the lumen of the endoplasmic reticulum (ER) where it both orchestrates cytoplasmic replication complex assembly and ER-Golgi virion maturation (23, 24, 38). NS1 is modified by N-linked glycosylation with high-mannose carbohydrates that direct dimerization (23–25, 40), and Golgi compartment processing of complex oligosaccharides facilitates NS1 secretion (40, 81). NS1 proteins from mosquito-borne FVs contain two conserved N-linked glycosylation sites (N130 and N207/208) (23, 25, 30, 82). In contrast, tick-borne FV NS1 proteins have three N-linked glycosylation sites (N85, N207/208, N223/224)(Fig. 2A and B) with two novel putative sites absent from other FVs (23, 83). The location of NxT sites on NS1 dimers is presented on putative POWV LI9 NS1 protein structures predicted using AlphaFold2 on the LI9 NS1 (Fig. 2B; Fig. S2).

Here, we used POWV reverse genetics to modify individual POWV NxS/T sites (N85Q, N208Q, or N224Q) to determine whether NS1 glycosylation affects viral replication and focal cell-to-cell spread. Using CPER, we split F2, containing NS1, into F2A and F2B using overlapping primers that contain glycosylation site-specific N->Q mutations (Fig. 2C). Amplified F2A and F2B fragments were substituted for F2 in CPERs and used to generate recLI9-NS1 NxT mutants, as in Fig. 1. Sequencing of rescued recLI9-NS1 mutants verified site-specific N->Q residue changes within NS1 proteins of each individual POWV (N85Q, N208Q, and N224Q) (Fig. S1). To investigate roles for NS1 NxT sites in NS1 expression and secretion, we infected VeroE6 cells at an MOI of 10 with the LI9-NS1-N85Q, LI9-NS1-N208Q, or LI9-NS1-N224Q mutant viruses. Intracellular and secreted NS1 proteins were evaluated 6 dpi by immunoblotting using an anti-NS1 mouse monoclonal antibody (Fig. 2D and E). Compared to WT LI9, mutating N208Q and N224Q glycosylation sites
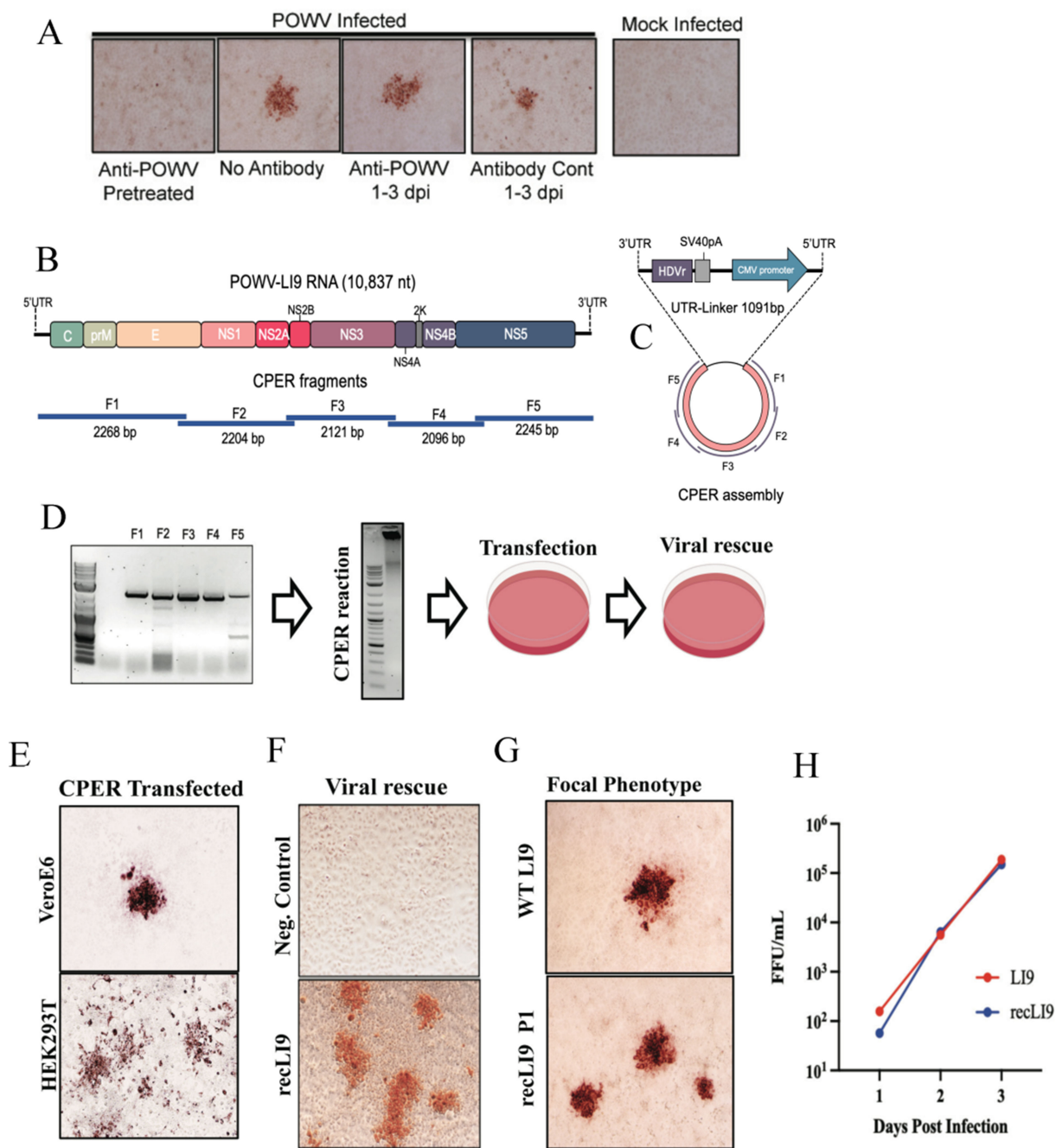
FIG 1 CPER generation and cell-to-cell spread of recombinant POWV strain LI9. (A) VeroE6 cells were infected with LI9 POWV at an MOI of 0.01 with or without anti-POWV HMAF (1:250) during adsorption. Cells were washed with PBS, and media were replaced with Dulbecco modified Eagle's medium (DMEM) with or without anti-POWV HMAF (1:250) or control ascitic fluid 6 h post adsorption. Cells were methanol fixed 3 dpi and immunostained with anti-POWV HMAF (1:5,000) (20, 79, 80). (B) Schematic of the LI9 POWV genome and overlapping fragments amplified from LI9 cDNA. (C) CPER assembly schematic of F1-F5 fragments with a UTR-Linker fragment containing the last 26 nucleotides of the LI9 3′UTR, hepatitis delta virus ribozyme (HDVr), SV40 polyadenylation signal, a cytomegalovirus (CMV) promoter, and 33 nucleotides of the LI9 5′UTR. (D) Agarose gel electrophoresis of PCR-amplified fragments (F1–F5) showing a representative image of three experimental repeats. F1–F5 were combined in equal molar amounts with the UTR-Linker in a CPER. A representative agarose gel of CPER product. Resultant LI9 CPER products were transfected into HEK293T or VeroE6 cells, and supernatants were subsequently used to infect VeroE6 cells and rescue infectious recLI9 viruses. (E) Immunostaining CPER-transfected VeroE6 or HEK293T cells (7 or 3 dpt, respectively) display focal cell-to-cell spread foci morphologies. (F) Infectious recLI9 virus rescued from CPER transfected cells and grown in HEK293T cells vs CPER controls amplified without the UTR-linker fragment. (G) Comparison of WT LI9 and recLI9 focal cell-to-cell spread phenotypes in immunostained VeroE6 cells. (H) Growth kinetics of WT LI9 (red) and recLI9 (blue) POWVs 1–3 dpi in VeroE6 cells (MOI 1). Analysis repeated at >3 times.
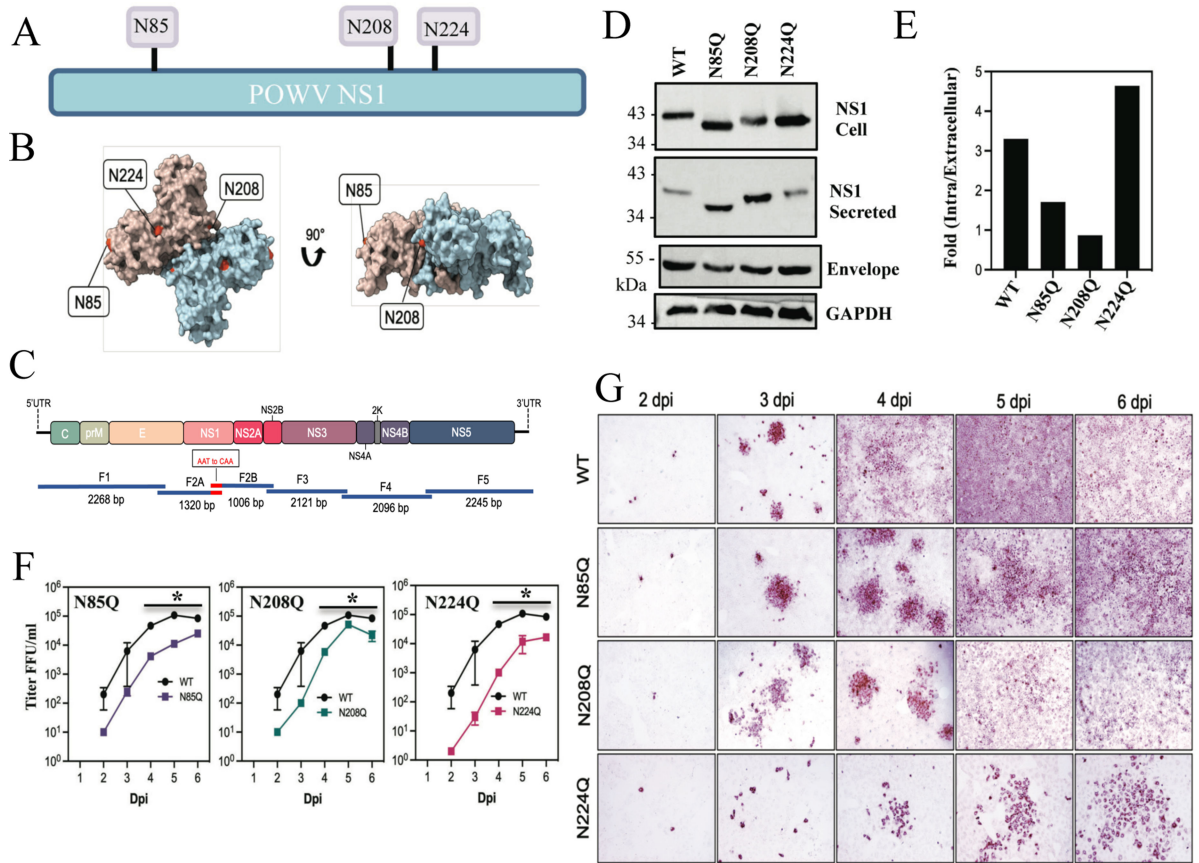
FIG 2 CPER POWV NS1 glycosylation mutants have impaired replication kinetics. (A) Schematic of N-linked glycosylation sites within POWV NS1 proteins. (B) Alphafold2 model of dimeric POWV NS1 protein showing pink or blue monomers and the localization of putative N-linked glycosylation sites (N85, N208, N224) in red (84). (C) Schematic strategy for CPER-generating N-linked glycosylation site (NxT) mutants using overlapping fragments to introduce N to Q codon changes. Fragment 2 was split into subfragments 2A and 2B with overlapping regions incorporating mutations. (D) VeroE6 cells were infected with WT LI9, recLI9-NS1$_{N85Q}$, recLI9-NS1$_{N208Q}$, and recLI9-NS1$_{N224Q}$ mutant viruses (MOI 1), and 7 dpi cell lysates and supernatants were analyzed by Western blot using antibodies POWV-NS1 (mAb), anti-POWV HMAF, or GAPDH. (E) Ratios of intracellular vs extracellular NS1 levels from representative Western blot (2D) of rec-LI9-NS1 glycosylation mutants were performed >2 times. (F) Growth kinetics of WT LI9 (black), CPER-generated NS1 glycosylation mutants recLI9-NS1$_{N85Q}$ (purple), recLI9-NS1$_{N208Q}$ (green), and recLI9-NS1$_{N224Q}$ (pink) 1–6 dpi of VeroE6 cells (MOI 0.1). *Statistically significant by two-way ANOVA with Tukey's post-test ($P < 0.05$). (G) Kinetic comparison of focal cell-to-cell spread by WT LI9 and recLI9-NS1 glycosylation mutants 1–6 dpi in VeroE6 cells (MOI 0.1) by anti-POWV (HMAF) immunoperoxidase staining of POWV-infected cells.

increased migration of NS1 proteins by Western Blot, while migration of NS1 from the N85Q mutant was dramatically increased from both intracellular and secreted NS1 sources (Fig. 2D). Evaluation of the relative amounts of intracellular and secreted NS1 proteins revealed a 200%–300% increase in the secretion of N85Q and N208Q NS1 proteins and a ~50% decrease in the secretion of the N224Q NS1 protein compared to NS1 from WT LI9 (Fig. 2E).

Relative to WT LI9 infection, titers of recLI9 NS1 glycosylation mutants revealed slower viral replication kinetics with maximal titers reduced by 1–3 logs from 2 to 6 dpi (Fig. 2F). While each NS1 glycosylation mutant spread focally, the formation of foci in monolayers was delayed by 1 day in N85Q and N208Q NS1 mutants (Fig. 2G). In contrast, foci formation was reduced by 2–3 days in the LI9-NS1-N224Q mutant, which failed to spread uniformly throughout monolayers by 6 dpi (Fig. 2G). These findings indicate that mutating any single LI9 NS1 glycosylation site reduced viral replication and spread, while mutating the NS1-N224Q glycosylation site resulted in a highly attenuated recLI9 mutant that was severely restricted in replication and spread *in vitro*.

Attempts to CPER generate recPOWV LI9 mutants with two glycosylation site changes (N85Q/N208Q, N85Q/N224Q, or N208Q/N224Q) failed to result in recovery of any double mutants. It remains unclear whether additional glycosylation site mutations critically impact NS1 functions required for POWV replication and virion assembly, and whether double mutants could be rescued by transcomplementation in NS1 protein-expressing cells.

POWV NS1 mutant dimerization, glycosylation, and secretion

Changing NS1 protein glycosylation may impact dimer formation, glycan processing, and NS1 protein functions. To determine whether dimer formation is altered in POWV NS1 glycosylation mutants, we compared untreated or heat-treated (2 min at 100°C) NS1 dimer stability prior to SDS-PAGE analysis. We found that all mutants formed dimers in unheated samples and that both dimers and monomers of glycosylation mutants were formed but with increased migration on SDS gels vs WT LI9 NS1 (Fig. 3A). These findings are consistent with unaltered dimer formation by DENV NS1 glycosylation site mutants (25).

We evaluated changes in high mannose or complex glycan addition to N-linked glycans of LI9 NS1 glycosylation mutants using endoglycosidases. Cell-associated and secreted NS1 proteins from WT and NxT mutants were treated with Endo H to remove high-mannose N-linked glycans or PNGase F to remove a combination of high mannose, hybrid, and complex oligosaccharides. Digestion profiles demonstrate that intracellular NS1 from WT LI9 or recLI9 glycosylation mutants possess mainly high-mannose N-linked glycans as digestion with either Endo H or PNGase F resulted in similar NS1 protein migration (Fig. 3B). However, secreted NS1 proteins of WT, N208Q, and N224Q are only partially reduced in size following Endo H digestion compared to PNGase (Fig. 3B), suggesting that N208Q and N224Q mutant NS1 glycans are further modified in the secretory pathway containing complex or hybrid sugars (Fig. 3B). In contrast, the secreted NS1 N85Q protein migrates similarly after Endo H or PNGase F digestion indicating that glycans on NS1 N85Q mutant proteins are not further processed in the Golgi (Fig. 3B). The large size difference of N85Q mutants, compared to NS1 proteins from LI9 WT or N208Q, and N224Q mutants suggests that the N85 glycosylation site determines whether N208 and N224 glycans are further processed during NS1 secretion.

Analysis of attenuated recLI9-NS1-N224Q in mice

POWV LI9 is lethal when intracranially or subcutaneously inoculated into C57BL/6 mice (20). Here, we assessed the lethality of *in vitro* attenuated recLI9-NS1-N224Q in murine models and found that like WT LI9, recLI9-NS1-N224Q is 100% lethal when i.c. inoculated into suckling mice ($N = 5$) 5–7 dpi. Although both WT LI9 and recLI9-N224Q are lethal when i.c. inoculated, there was a 1-day difference in the timing of lethality between WT and mutant (Fig. 4A and B). As i.c. inoculation of suckling mice reflects neurovirulence, but not neuroinvasion, we s.c. inoculated C57BL/6 mice with LI9 or recLI9-NS1-N224Q ($N = 8$–10) and evaluated weight loss and lethality from 1 to 20 dpi. WT LI9 caused weight loss and was lethal in 40% of C57BL/6 mice 9–12 dpi. In contrast, in mice, s.c. inoculated with recLI9-NS1-N224Q lethal disease onset was delayed, with 80% of mice surviving infection (Fig. 4B and C). Similar to attenuating replication and spread kinetics *in vitro*, our findings suggest that mutating the N224Q glycosylation site in infectious LI9 is attenuating *in vivo* and partially reduces lethal POWV outcome.

Generation of an infectious POWV Split11-GFP reporter virus

Recombinant viruses expressing fluorescent proteins permit live cell, real time, analysis of cellular protein interactions, viral protein trafficking, and the development of high-throughput screens for viral inhibitors (64, 66, 69, 71, 73, 74, 85, 86). Expressing the 11thβ-strand of green fluorescent protein (GFP11-residues 215–230) with co-expressed GFP$_{1-10}$ (residues 1–214) reconstitutes a fluorescent GFP molecule (Fig. 5A) (69, 70, 72).
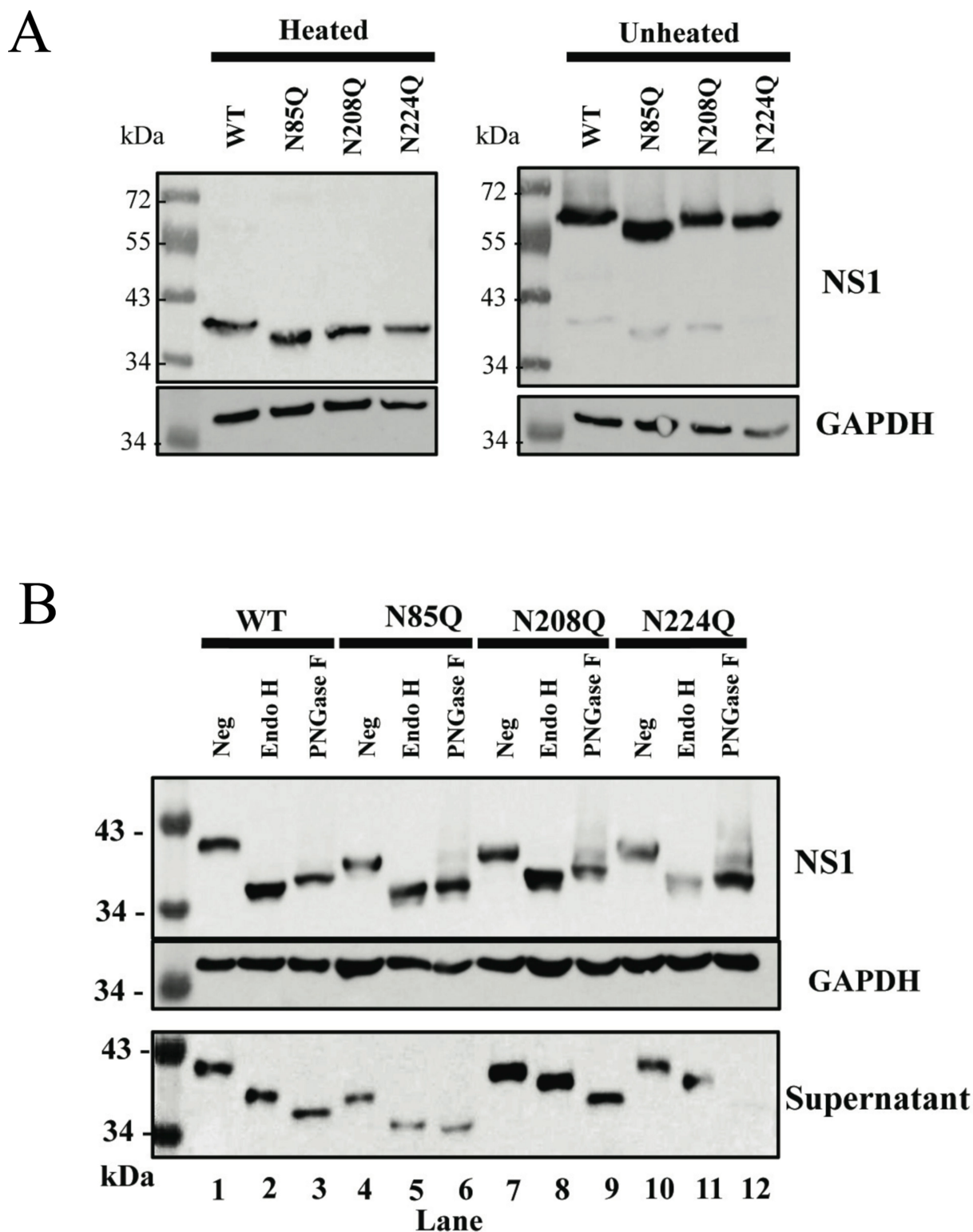
FIG 3 POWV NS1 mutant dimerization and glycosidase analysis. (A) VeroE6 cells were infected with WT POWV LI9, recLI9-NS1$_{N85Q}$, recLI9-NS1$_{N208Q}$, or recLI9-NS1$_{N224Q}$ mutants (MOI, 1). Cell lysates were harvested 7 dpi with or without heat-directed dimer disassembly prior to Western blot analysis using anti-POWV-NS1 mAb (1:5,000) or anti-GAPDH (1:5,000). (B) VeroE6 cells were infected with WT LI9, recLI9-NS1$_{N85Q}$, recLI9-NS1$_{N208Q}$, or recLI9-NS1$_{N224Q}$ mutant viruses (MOI, 1). Cell lysates were harvested 7 dpi, and 20 µg of protein lysate or 50 µL of supernatant was subjected to Endo H or PNGase F digestion. Undigested and digested samples from cell lysate or supernatant were analyzed by Western blot using antibody to POWV-NS1 or GAPDH.
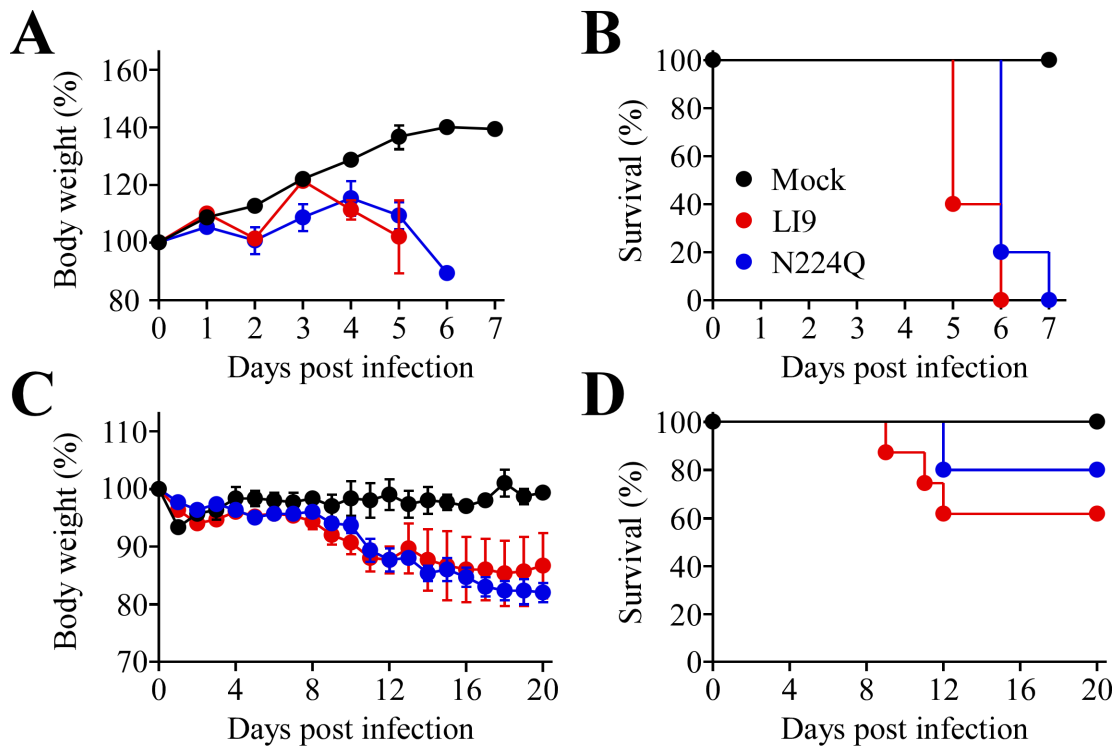
FIG 4 POWV N224Q mutation attenuates neurovirulence in C57BL/6 mice. (A) Body weight analysis and (B) Kaplan-Meier survival curves (LI9 vs recLI9-N224Q, P = 0.0442) of pups of C57BL/6 mice (N = WT:5; N224Q:5; Cont:3) intracranially inoculated with 2×10^2 FFU of WT LI9, recLI9-N224Q, or buffer only. (C) Body weight analysis and (D) Kaplan-Meier survival curves (LI9 vs N224Q, P = 0.3310, not significant) for C57BL/6 mice (male, N = WT:8; N224Q:10; Cont:4) footpad inoculated with 2×10^3 FFU of WT LI9, recLI9-N224Q, or a buffer-only control.

As a means of analyzing POWV NS1 protein functions, we used CPER to generate NS1 C-terminally tagged with a split GFP11 fusion protein in recLI9 (recLI9-GFP11) (Fig. 5B). The recLI9-GFP11 reporter virus forms infected cell foci by immunostaining and replicates with similar kinetics and titers 1–3 dpi as WT LI9 in VeroE6 cells (Fig. 5C and D). HEK293T and VeroE6 cells were transduced with retroviruses expressing cytoplasmic GFP_{1-10} and mCherry (mCh-GFP_{1-10}) or an ER-translocated GFP_{1-10}-KDEL and cytoplasmic mCherry (mCh-ER-GFP_{1-10}). We infected mCh-GFP_{1-10} or mCh-ER-GFP_{1-10}-expressing HEK293T cells with the recLI9-NS1-GFP11 virus and found GFP-positive infected cell foci in ER-GFP_{1-10} but not in GFP_{1-10}-expressing cells 2–3 dpi (Fig. 5E; Fig. S3). Similarly, in VeroE6 cells expressing mCh-ER-GFP_{1-10}, infection with recLI9-NS1-GFP11 reconstituted NS1-GFP fluorescence with a perinuclear localization consistent with NS1-GFP11 translocation to the ER (Fig. 5F). In addition, we found abundant expression of NS1-GFP11 in large fluorescent vesicles (6 dpi) that may reflect NS1 protein accumulation in intracellular secretory or specialized vesicles. Intracellular NS1 accumulation provides a rationale for reduced NS1 secretion during POWV infection and suggests that novel vesicular trafficking may foster cell-to-cell spread in POWV-infected cells. Collectively, using CPER reverse genetics, we have generated an infectious recLI9-GFP11 reporter virus that provides a mechanism for analyzing the role of NS1 in restricting POWV secretion or directing cell-to-cell spread and provides an infectious fluorescent reporter virus that can be used to screen POWV inhibitors.

DISCUSSION

We isolated the LI9 strain of POWV directly from ticks in VeroE6 cells in order to avoid potential neuroadaptive changes of prototype POWV strains (LB and SP) that were isolated and adapted to growth in murine brains (5, 6, 14, 20). The LI9 POWV isolate nonlytically infects VeroE6 cells, unexpectedly spreading focally in cells lacking restrictive
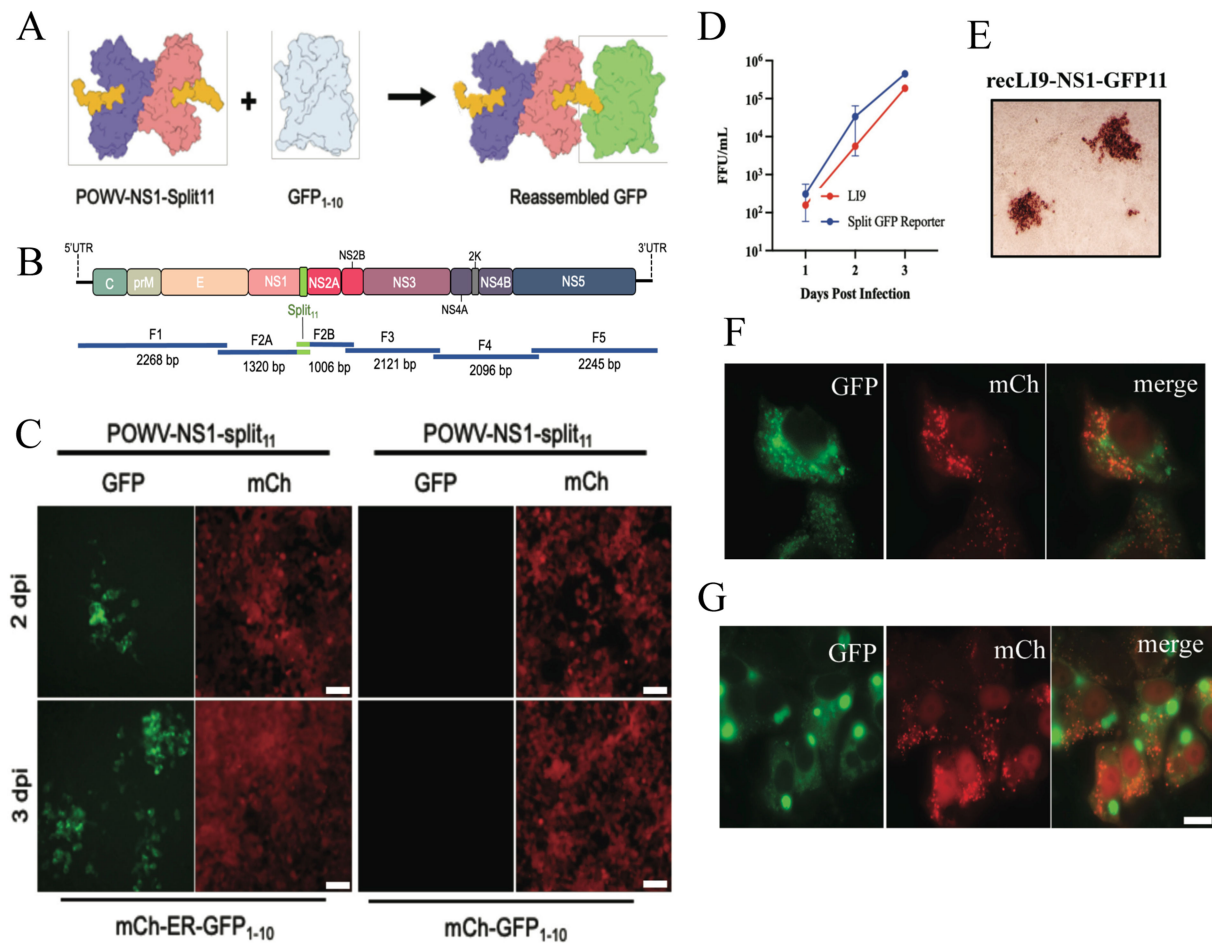
FIG 5 Generation of a split GFP POWV reporter virus. (A) Schematic of the split GFP fluorescence reporter system directed by the recLI9-NS1-GFP11 virus. Individual NS1 monomers (blue and pink) with a 16 residue GFP11 tag added to the NS1 C-terminus (yellow) with co-expressed, nonfluorescent, GFP$_{1-10}$ (gray). The recLI9-NS1-GFP11 expression of NS1-GFP11 protein reconstitutes GFP fluorescence in cells co-expressing GFP$_{1-10}$. (B) CPER strategy for POWV-NS1-split11 generation. F2 was split into subfragments F2A and F2B with primer-directed incorporation of GFP11 sequences. (C) Retrovirus-transduced HEK293T cells constitutively expressing mCherry (cytoplasm) and either ER-localized ER-GFP$_{1-10}$ (mCh-ER-GFP$_{1-10}$) or cytoplasm-localized GFP$_{1-10}$ (mCh-GFP$_{1-10}$) were infected with recLI9-NS1-GFP11. Live imaging captured 2–3 dpi shows foci of GFP fluorescence in LI9-NS1-GFP11-infected cells expressing ER translocated GFP$_{1-10}$ but not cytoplasmically expressed GFP$_{1-10}$. (D) Growth kinetics of WT LI9 (red) and recLI9-NS1-GFP11 (blue) 1–3 dpi in VeroE6 cells (MOI 1). (E) Immunostaining of LI9-NS1-GFP11 infected VeroE6 cell foci 3 dpi with anti-POWV HMAF. (F and G) Retrovirus-transduced VeroE6 cells expressing mCherry-ER-GFP$_{1-10}$ were LI9-NS1-GFP11 infected, and 6 dpi cells paraformaldehyde fixed. Representative images show perinuclear NS1-GFP fluorescence (F) and the discrete accumulation of NS1-GFP in large intracellular vesicles 6 dpi (G). Bars represent 10 µm.

overlays (20). LI9 spread focally in media containing high levels of anti-POWV-neutralizing antibodies, revealing that LI9 spreads cell-to-cell without requiring apical release into cell supernatants (Fig. 1). This both confirms the large cell-associated nature of POWVs (6), while uniquely mirroring data establishing that HCV, a distantly related FV, spreads cell-to-cell in hepatocytes (75–78). The neutralizing antibody-independent, cell-to-cell spread of HCV is proposed to occur at partially sealed cell junctions that permit HCV to evade immune surveillance (75–78). Measles virus (MV) was also shown to spread cell-to-cell in epithelial cells, without syncytia formation, using a GFP reporter virus (87). The MV-GFP reporter was visualized flowing to the cytoplasm of adjacent cells through lateral pores and was suggested as a mechanism for MV transmission from epithelial cells to neurons (78, 87). Implying that POWV cell-to-cell spread is epithelial cell specific, we found that POWV fails to spread cell-to-cell in hBMECs or pericytes. At later times post-infection, POWV titers increase and spreads conventionally by the diffusion of cell-free viral particles (78). Cell-to-cell spread is a known viral mechanism for immune evasion

(78) that may contribute to dissemination in the skin or foster CNS transmission via epithelial cell barriers that comprise the choroid plexus (88–90). The mechanism of POWV cell-to-cell spread remains to be defined, and our recLI9-GFP reporter virus may permit analysis of POWV trafficking and spread to recipient cells.

In order to define mechanisms for attenuating POWVs, we developed a CPER reverse genetics system that authentically generates infectious recombinant POWVs. The CPER approach bypasses stability issues of bacterial FV clones and creates recombinant POWVs from amplified POWV genomic cDNAs and clones (38, 60–63, 67). The recLI9 POWV was CPER generated by circularizing five to seven fragments of LI9 cDNAs with defined CMV promoter and HDVr-directed 5′ and 3′ termini. CPER-assembled LI9 DNA transfected into HEK or VeroE6 cells results in infectious recLI9 progeny that differs only by cell transfection efficiency. The authenticity of recLI9 viruses with WT LI9 was verified by sequencing, replication kinetics, and phenotypically by focal cell-to-cell spread (Fig. 1 and 2).

Our newly developed POWV CPER reverse genetics system permits us to define determinants of POWV spread, neuroinvasion, and neurovirulence, providing a mechanism for genetically attenuating POWVs and rationally designing live attenuated POWV vaccines. Reverse genetics has been accomplished for several FVs, initially using RNA transcription or plasmid approaches and more recently by employing CPER systems (38, 60–63, 67). Reverse genetics has also been used to generate chimeric FVs with prM-Env-specific neutralization determinants and NS protein backgrounds derived from attenuated FVs or the Yellow Fever Virus (YFV) 17D vaccine (23, 46, 52, 68). Insertion of the POWV prM-Env in a YFV-17D background retained lethal neurovirulence with only 43% of inoculated mice surviving this virulent chimera (51).

Mutating FV envelope and NS1 protein glycosylation sites have been associated with reduced replication and neuroinvasion (27–29, 91–94). However, how glycosylation alters FV virulence is likely dependent on both Env and NS1 functions that in combination determine FV assembly, spread, and tissue tropism (47). FV NS1 proteins are reported to regulate viral replication, particle formation, and functions of secreted extracellular NS1. Mutating residues 160 and 273 of the JEV NS1 protein regulate replication and particle formation, while mutating YFV or DENV NS1 N130 glycosylation sites reduces viral yield *in vitro* and neurovirulence following i.c. inoculation of mice (37, 46). In contrast, multiple mutations around NS1 glycosylation sites were required for WNV attenuation (48, 95).

POWV contains two novel NS1 glycosylation sites, not found in mosquito-borne FVs, and adds complex glycans to unique sites on the periphery of putative NS1 hexamers (Fig. S2). To define POWV NS1 glycosylation functions, we modified individual NS1 glycosylation sites (N85Q, N208Q, and N224Q) and isolated infectious recLI9 NS1 mutant POWVs (Table S1). Each glycosylation site mutant spread focally cell-to-cell in VeroE6 cells like parental LI9 but with a 1–2 log decrease in NS1 mutant titers and reduced replication kinetics. A pronounced 2- to 3-day reduction in the timing of foci formation by the recPOWV-NS1-N224Q mutant coincides with reduced replication and reveals a severely attenuated *in vitro* phenotype. Although i.c. inoculation of mice with the NS1-N224Q glycosylation mutant was lethal, peripheral inoculation of the recLI9-NS1-N224 mutant resulted in 80% survival, elicited antibody responses to POWV Env proteins, and a partially attenuated phenotype relative to WT LI9 infection. Further analysis is needed to determine if the NS1-N224Q glycosylation mutant is attenuated at peripheral spread or neuroinvasive levels and how the unique structural position of the POWV NS1 N224 glycosylation site restricts replication and delays POWV cell-to-cell spread. Irrespective of the mechanism, our findings rationalize including N224Q mutations in strategies for developing a live attenuated POWV vaccine.

Mutating WNV NS1 glycosylation sites (N130, N207) produced stable attenuated strains with NS1 accumulation in the ER and restricted NS1 secretion (48, 95). In DENV NS1, N207 mutants showed reduced dimer stability and secretion, with complex glycans attached to N130 and high mannose glycans added to N207 (23, 25). The NS1 N85 glycosylation site was reported to be broadly required for high mannose or complex

glycan processing, suggesting that N85Q mutations broadly restrict Golgi processing of N208/N224 glycans and alter NS1 secretion (30). Although all single POWV LI9 NS1 glycosylation mutants formed dimers and were secreted from cells, NS1 secretion was reduced in N224Q mutants and increased in NS1 N85Q and N208Q mutants relative to WT LI9. It remains to be determined how the position of individual glycosylation sites (Fig. 2B; Fig. S2) impacts higher order NS1 glycan processing or hexamer formation or constrains NS1 secretion and POWV release from cells.

Why some NS1s are highly secreted, while others remain highly cell associated, and how NS1 proteins regulate the assembly and secretion of FVs remains an enigma linked to viral spread and pathogenic mechanisms (2, 23, 32, 41, 96). POWV virions (6) and NS1 proteins remain highly cell associated with low levels of secreted NS1, and this novel NS1 attribute may have a role in directing the unique cell-to-cell spread phenotype of POWVs. Many functions ascribed to NS1 do not reflect that NS1 proteins are cotranslationally translocated into ER compartments and unavailable for cytoplasmic interactions (2, 23, 32). Further, NS1 and Env proteins that are both present in secretory vesicles, yet discretely released from cells, suggest intertwined roles for NS1 and Env glycosylation in virion assembly or secretion that have yet to be discovered (27, 38, 41, 96).

As an initial approach to study POWV NS1 translocation and secretion, we used CPER to generate a recLI9-NS1-GFP11 reporter virus for analysis of NS1 localization in cells. Fluorescence of the recPOWV NS1 split GFP11 protein was reconstituted in the ER of cells expressing ER-GFP$_{1-10}$ protein. This demonstrates the ability of recLI9-NS1-GP11 to serve as a fluorescent reporter virus and permits real-time analysis of POWV infection and NS1 functions in the lumen of the ER (69, 71, 97). Initial studies demonstrate the ER localization of NS1-GFP fluorescence and the novel accumulation of NS1-GFP in large intracellular vesicles in infected cells 6 dpi. These findings reveal NS1 lined vesicles and suggest a mechanism for NS1 retention that may restrict assembled POWV particle release (6) or contribute to a vesicular mechanism of POWV cell-to-cell spread. The nature of NS1 fluorescing vesicles (secretory, lipid droplet, autophagosome, convoluted membranes) remain to be defined (24, 25, 32, 41, 47, 48, 95, 96) but may explain how NS1 proteins are excluded from virions within secretory vesicles, yet determine FV spread in mammalian cells (38, 98, 99). Combining NS1 glycosylation mutants in a LI9-NS1-GFP reporter background may reveal roles for NS1 glycosylation sites in POWV secretion that impact attenuation. Further, the production of an infectious POWV NS1-GFP reporter virus provides a platform for high-throughput screening of POWV replication inhibitors (64, 66, 86, 97).

Our findings provide a robust mechanism for generating recombinant POWV mutants and defining determinants of cell-to-cell spread, neuroinvasion, and neurovirulence *in vitro* and *in vivo*. We generated a viable infectious POWV reporter virus that permits analysis of NS1 functions required for viral replication, maturation, and neurovirulence and revealed an NS1-N224Q glycosylation mutation that attenuates POWV replication *in vitro* and partially attenuates POWV in mice. Studies presented provide a mechanism for assessing attenuating POWV mutations and genetically designing live attenuated POWV vaccines.

MATERIALS AND METHODS

Cells and virus

Human embryonic kidney 293T cells (HEK293T) and Vero E6 cells were maintained in Dulbecco modified Eagle's medium (Gibco) with 8% fetal bovine serum (FBS), 10,000 U/mL of penicillin, and 10,000 µg/mL of streptomycin (Gibco, USA), and following viral infection, in media with 2% FBS. POWV strain LI9 (GenBank accession: MZ576219) was isolated from infected *Ixodes scapularis* ticks in VeroE6 cells and passaged three to four times in VeroE6 cells (20, 79). Work with infectious LI9 POWV and CPER-generated

recombinant LI9 POWVs (recLI9) was performed in a certified BSL3 facility at Stony Brook University.

Viral RNA extraction and cDNA synthesis

RNA from POWV-infected VeroE6 cells was RLT extracted and RNeasy column (Qiagen) purified. cDNA synthesis was performed using the Transcriptor first-strand cDNA synthesis kit (Roche) following the manufacturer's protocol and a primer complimentary to the 3′UTR (Table S2, oligo F5R) (20, 79, 80).

PCR amplification of DNA fragments and CPERs

Five POWV-LI9 fragments were amplified from viral cDNA (Fig. 1A and B) using high-fidelity Phusion polymerase (NEB) and corresponding paired primers (Table S2) that have a complementary 26-nucleotide overlap. An additional PCR fragment (UTR linker) was generated from plasmid pMiniT containing the CMV promoter, the first and the last 26 nts of the POWV-LI9 sequence, an HDVr, and SV40 polyadenylation site. POWV cDNA was amplified into six individual POWV DNA fragments: initial denaturation 98℃ for 30 s; 32 cycles of 98℃ for 20 s, 60℃ for 30 s, and 72℃ with 30 s per kb; and a final extension at 72℃ for 5 min. Resulting fragments were gel purified, Monarch kit (NEB) extracted, and 0.1 pmol of each DNA fragment was CPER amplified in a 50-μL reaction containing 200 μM of dNTPs, 1× Phusion polymerase GC reaction buffer, and 1 μL Phusion polymerase. The following cycling conditions were used: initial denaturation 98℃ for 30 s; 12 cycles of 98℃ for 20 s, 60℃ for 30 s, and 72℃ for 10 min; and a final extension at 72℃ for 10 min. CPERs lacking the UTR-Linker fragment were generated and used as negative controls.

For generating POWV-NS1$_{N85Q}$, NS1$_{N208Q}$, and NS1$_{N224Q}$ mutant viruses, subfragments of fragment F2 (F2A, F2B) were generated by PCR from LI9 POWV cDNA, with primers containing AAC to CAA codon changes (Table S2) to generate NS1 proteins containing N85Q, N208Q, or N224Q mutations. Subfragments F2A and F2B replaced F2 in CPERs as above. For generating the recLI9-NS1-Split$_{11}$ reporter virus, subfragments of fragment F2 were similarly amplified from LI9 cDNA using primers containing Split$_{11}$ sequences (Table S2) and used in CPERs as above.

CPER transfection and RecLI9 virus rescue

CPERs were Monarch kit purified, eluted in sterile H$_2$O, and transfected into HEK293T cells seeded in 12-well plates using Lipofectamine 3000 reagent (Invitrogen) (20, 79, 80). Two days post-transfection, supernatants were harvested and amplified in VeroE6 cells to generate viral stocks and compared to transfection of control CPERs. Total RNA from VeroE6 cell infections with recLI9, recLI9 -NS1$_{N85Q}$, -NS1$_{N208Q}$, and -NS1$_{N224Q}$ mutant viruses, and recLI9-NS1-GFP11 reporter virus was purified using RNeasy kit (Qiagen). cDNA synthesis was performed as above using random hexamer primers (25℃ for 10 min, 50℃ for 60 min, and 90℃ for 5 min). Mutants were completely sequenced as described (20) in the SBU Genomics facility.

POWV LI9 infection and immunostaining

WT LI9 POWV, recLI9, recLI9-NS1$_{N85Q}$, recLI9-recNS1$_{N208Q}$, and recNS1$_{N224Q}$ mutant viruses were adsorbed to ~60% confluent VeroE6 cells for 1 h. Following adsorption, monolayers were washed with phosphate buffered saline (PBS) and grown in DMEM-2% FBS. Viral titers were determined by focus assay following serial dilution and infection of VeroE6 cells and quantifying infected cells 24 hpi by immunostaining with anti-POWV hyperimmune mouse ascites fluid (HMAF; 1:5,000 [ATCC]), HRP-labeled anti-mouse IgG (1:3,000; KPL-074–1806), and AEC staining as previously described (20).

Western blotting

VeroE6 cells were infected with WT LI9 or recLI9 mutant viruses (MOI, 1), and cells were harvested at 7 dpi in lysis buffer containing 1% NP-40 (150 mM NaCl, 50 mM Tris-Cl, 10% glycerol, 2 mM EDTA, 10 nM sodium fluoride, 2.5 mM sodium pyrophosphate, 2 mM sodium orthovanadate, 10 mM β-glycerophosphate) with 1× protease inhibitor cocktail (Sigma). Total protein levels were determined in a bicinchoninic acid assay (Thermo Scientific), and 20 µg of protein was resolved by SDS-10% polyacrylamide gel electrophoresis. Proteins were transferred to nitrocellulose, blocked in 5% bovine serum albumin, and incubated with the indicated antibodies. Antibodies used were mouse anti-POWV NS1 (M837; Native Antigen Company) (1:5,000), anti-POWV HMAF sera (ATCC) (1:1,000), and anti-GAPDH (G9545; Sigma-Aldrich) (1:5,000) (20, 79, 80). Protein was detected using HRP-conjugated anti-mouse secondary antibody (Amersham) and Luminata Forte Western HRP substrate (Millipore).

Glycosidase analysis

VeroE6 cells were infected with LI9, recLI9-NS1$_{N85Q}$, recLI9-NS1$_{N208Q}$, and recLI9-NS1$_{N224Q}$ mutant viruses (MOI, 1) and harvested 7 dpi. Cells were washed with PBS and lysed in 1% NP-40 buffer as above, and 20 µg of lysate or 50 µL of supernatants was subjected to Endo H (P0702S NEB) or PNGase F (P0709S NEB) digestion following the manufacturer's protocols. Samples were resolved by SDS-10% polyacrylamide gel electrophoresis and Western blotted (20, 79, 80), and viral NS1 protein was detected using mouse anti-POWV NS1 (M837; Native Antigen Company) as above.

Retrovirus GFP$_{1-10}$ vectors

Retrovirus vectors were generated by transfecting HEK293T or VeroE6 cells using polyethylenimine (PEI) transfection using a DNA/PEI ratio of 1:3 (100). HEK293T cells (3.8 × 10^6) were preincubated with 25 µM chloroquine diphosphate for 5 h and transfected with pQCXIP-mCh-2A-ER-GFP$_{1-10}$ or pQCXIP-mCh-2A-GFP$_{1-10}$ plasmids with packaging plasmids pMMLV-CMV-GagPol and pLP/VSVG using in a 3:2:1 ratio. After 18 h, media were replaced, and the viral supernatants were harvested 72 hpt and filtered through a 0.45-µm PVDF filter.

Live cell POWV fluorescence

Packaged retroviruses, mCh-2A-ER-GFP$_{1-10}$ or mCh-2A-GFP$_{1-10}$, were used to transduce ~50% confluent monolayers of VeroE6 or HEK293T cells to constitutively express mCherry-ER-GFP$_{1-10}$ or mCherry-GFP$_{1-10}$. After 2 days, cells were selected using puromycin (5 or 0.5 µg/mL, respectively, for VeroE6 and HEK293 cells) for 2 days. Puromycin-selected cells were infected with recLI9-NS1-GFP11 (MOI 5) in microslides chambers (IblTreat, Germany), and live-cell fluorescence was monitored using a Nikon Axiovert microscope in the BSL3. Additionally, infected VeroE6 were fixed for 1 h in 1% paraformaldehyde and washed three times with PBS, and fluorescence was measured using EVOS M5000 microscope with a 60× oil immersion objective. Control for split-GFP system specificity was performed by PEI co-transfection of pQCXIP-mTag-ER-split11 or pQCXIP-mTag-split11 with pQCXIP-mCh-2A-ER-GFP$_{1-10}$ into ~50% confluent HEK293T. Fluorescence was observed 2 days post-transfection using Olympus IX51 microscope and Olympus DP71 camera (Fig. S3).

LI9 POWV NS1 molecular modeling

The 3D model of dimeric LI9 NS1 protein was obtained using multimer prediction in AlphaFold2 using ColabFold within ChimeraX 1.5 software (100). Five models were created with the top-scoring model selected after relaxation. The POWV LI9 NS1 hexamer model was generated using cryoEM structures from DENV2 soluble NS1 hexamers (PDB 7WUV) scaffolding with the model relaxed using Rosetta Relax (101, 102).

In vivo LI9 POWV infection experiments

Anesthetized murine C57BL/6 pups (<2-week old, N = 3–5) were intracranially infected with 2×10^2 FFU POWV or buffer-only control in a volume of 2 L. Infected mice were monitored twice daily for signs of disease and daily for weight loss. Peripheral inoculation: C57BL/6 mice (male, 41- to 51-week-old, N = 4–10, Jackson Laboratory) were anesthetized via intraperitoneal injection with 100 mg mL^{-1} (1) of ketamine and 20 mg mL^{-1} (1) of xylazine per kilogram of body weight. Animals were infected via subcutaneous footpad injection with 2×10^3 FFU POWV or buffer-only control in a volume of 20 L. Weights and neurovirulent sequelae were monitored daily as indicated.

Biosafety and biosecurity

Animal research was performed in accordance with institutional guidelines following experimental protocol review, approval, and supervision by the Institutional Biosafety Committee and the Institutional Animal Care and Use Committee at Stony Brook University. Animals were managed by the Division of Laboratory Animal Resources (Stony Brook University), which is accredited by the American Association for Accreditation of Laboratory Animal Care and the Department of Health and Human Services. Animals were maintained in accordance with the applicable portions of the Animal Welfare Act and the DHHS "Guide for the Care and Use of Laboratory Animals." Veterinary care was under the direction of full-time resident veterinarians boarded by the American College of Laboratory Animal Medicine. Experiments with infectious POWV were performed in an ABSL3 facility at SBU.

AUTHOR AFFILIATIONS

[1]Department of Microbiology and Immunology, Stony Brook University, Stony Brook, New York, USA
[2]School of Chemistry and Molecular Biosciences, University of Queensland, St Lucia, Queensland, Australia
[3]Molecular and Cell Biology Program, Stony Brook University, Stony Brook, New York, USA
[4]Microbiology and Molecular Epidemiology Division, Environmental Health Institute, National Environmental Agency, Singapore, Singapore
[5]Center for Infectious Disease, Stony Brook University, Stony Brook, New York, USA

AUTHOR ORCIDs

Jonas N. Conde ⓘ http://orcid.org/0000-0001-5895-1114
Hwan Keun Kim ⓘ http://orcid.org/0000-0003-2095-9705
Erich R. Mackow ⓘ http://orcid.org/0000-0001-9156-1222

AUTHOR CONTRIBUTIONS

Grace E. Himmler, Conceptualization, Data curation, Formal analysis, Investigation, Methodology, Validation, Visualization, Writing – original draft, Writing – review and editing | Megan C. Mladinich, Investigation, Methodology, Validation, Visualization, Writing – review and editing | Yin Xiang Setoh, Conceptualization, Formal analysis, Methodology | Alberto A. Amarilla, Conceptualization, Formal analysis, Methodology | Nicholas Saladino, Investigation, Methodology, Resources | Elena E. Gorbunova, Investigation, Methodology, Validation, Resources, Project administration, Supervision | Daniel J. Salamango, Conceptualization, Investigation, Methodology, Validation, Writing – review and editing, Resources, Supervision | Jorge Benach, Conceptualization, Investigation, Methodology, Writing – review and editing, Resources, Project administration, Supervision, Funding acquisition | Hwan Keun Kim, Conceptualization, Data curation, Formal analysis, Investigation, Methodology, Validation, Writing – original draft, Writing – review and editing, Resources, Project administration, Supervision, Funding acquisition | Erich R. Mackow, Conceptualization, Data curation, Formal analysis, Investigation, Methodology, Validation, Writing – original draft, Writing – review and editing, Resources, Project administration, Supervision, Funding acquisition.

DIRECT CONTRIBUTION

This article is a direct contribution from Jorge Benach, a Fellow of the American Academy of Microbiology, who arranged for and secured reviews by Christopher Basler, Icahn School of Medicine at Mount Sinai, and Harry Greenberg, Stanford University.

ADDITIONAL FILES

The following material is available online.

Supplemental Material

Fig. S1 (mBio01388-23-S0001.tif). Sequencing chromatograms.
Fig. S2 (mBio01388-23-S0002.tif). POWV NS2 hexamer model.
Fig. S3 (mBio01388-23-S0003.tif). Specific reconstitution of GFP.
Supplemental material (mBio01388-23-S0004.docx). Table S1, Table S2, and legends to Fig. S1 to S3.

REFERENCES

1. Kemenesi G, Bányai K. 2019. Tick-borne flaviviruses, with a focus on Powassan virus. Clin Microbiol Rev 32:e00106-17. https://doi.org/10.1128/CMR.00106-17
2. Pierson TC, Diamond MS. 2020. The continued threat of emerging flaviviruses. Nat Microbiol 5:796–812. https://doi.org/10.1038/s41564-020-0714-0
3. Hermance ME, Thangamani S. 2017. Powassan virus: an emerging arbovirus of public health concern in North America. Vector Borne Zoonotic Dis 17:453–462. https://doi.org/10.1089/vbz.2017.2110
4. Ebel GD, Kramer LD. 2004. Short report: duration of tick attachment required for transmission of Powassan virus by deer ticks. Am J Trop Med Hyg 71:268–271.

5. McLEAN DM, DONOHUE WL. 1959. Powassan virus: isolation of virus from a fatal case of encephalitis. Can Med Assoc J 80:708–711.

6. ABDELWAHAB KS, ALMEIDA JD, DOANE FW, MCLEAN DM. 1964. Powassan virus: morphology and cytopathology. Can Med Assoc J 90:1068–1072.

7. McLean DM, Smith PA, Livingstone SE, Wilson WE, Wilson AG. 1966. Powassan virus: vernal spread during 1965. Can Med Assoc J 94:532–536.

8. Fatmi SS, Zehra R, Carpenter DO. 2017. Powassan virus-A new reemerging tick-borne disease. Front Public Health 5:342. https://doi.org/10.3389/fpubh.2017.00342

9. Feder HM, Telford S, Goethert HK, Wormser GP. 2021. Powassan virus encephalitis following brief attachment of connecticut deer ticks. Clin Infect Dis 73:e2350–e2354. https://doi.org/10.1093/cid/ciaa1183

10. Telford SR, Armstrong PM, Katavolos P, Foppa I, Garcia AS, Wilson ML, Spielman A. 1997. A new tick-borne encephalitis-like virus Infecting New England deer ticks, Ixodes dammini. Emerg Infect Dis 3:165–170. https://doi.org/10.3201/eid0302.970209

11. Brackney DE, Nofchissey RA, Fitzpatrick KA, Brown IK, Ebel GD. 2008. Stable prevalence of Powassan virus in Ixodes scapularis in a northern wisconsin focus. Am J Trop Med Hyg 79:971–973. https://doi.org/10.4269/ajtmh.2008.79.971

12. Anderson JF, Armstrong PM. 2012. Prevalence and genetic characterization of Powassan virus strains infecting Ixodes scapularis in connecticut. Am J Trop Med Hyg 87:754–759. https://doi.org/10.4269/ajtmh.2012.12-0294

13. Ebel GD. 2010. Update on Powassan virus: emergence of a North American tick-borne flavivirus. Annu Rev Entomol 55:95–110. https://doi.org/10.1146/annurev-ento-112408-085446

14. Ebel GD, Foppa I, Spielman A, Telford SR. 1999. A focus of deer tick virus transmission in the northcentral United States. Emerg Infect Dis 5:570–574. https://doi.org/10.3201/eid0504.990423

15. Ebel GD, Spielman A, Telford SR. 2001. Phylogeny of North American Powassan virus. J Gen Virol 82:1657–1665. https://doi.org/10.1099/0022-1317-82-7-1657

16. McLean DM, Ladyman SR, Purvin-Good KW. 1968. Westward extension of Powassan virus prevalence. Can Med Assoc J 98:946–949.

17. Pesko KN, Torres-Perez F, Hjelle BL, Ebel GD. 2010. Molecular epidemiology of Powassan virus in North America. J Gen Virol 91:2698–2705. https://doi.org/10.1099/vir.0.024232-0

18. Campbell O, Krause PJ. 2020. The emergence of human Powassan virus infection in North America. Ticks Tick Borne Dis 11:101540. https://doi.org/10.1016/j.ttbdis.2020.101540

19. Sanchez-Vicente S, Tagliafierro T, Coleman JL, Benach JL, Tokarz R. 2019. Polymicrobial nature of tick-borne diseases. mBio 10:e02055-19. https://doi.org/10.1128/mBio.02055-19

20. Conde JN, Sanchez-Vicente S, Saladino N, Gorbunova EE, Schutt WR, Mladinich MC, Himmler GE, Benach J, Kim HK, Mackow ER. 2022. Powassan viruses spread cell to cell during direct isolation from Ixodes ticks and persistently infect human brain endothelial cells and pericytes. J Virol 96:e0168221. https://doi.org/10.1128/JVI.01682-21

21. Mukhopadhyay S, Kim B-S, Chipman PR, Rossmann MG, Kuhn RJ. 2003. Structure of West Nile virus. Science 302:248. https://doi.org/10.1126/science.1089316

22. Kuhn RJ, Zhang W, Rossmann MG, Pletnev SV, Corver J, Lenches E, Jones CT, Mukhopadhyay S, Chipman PR, Strauss EG, Baker TS, Strauss JH. 2002. Structure of dengue virus: implications for flavivirus organization, maturation, and fusion. Cell 108:717–725. https://doi.org/10.1016/s0092-8674(02)00660-8

23. Carpio KL, Barrett ADT. 2021. Flavivirus NS1 and its potential in vaccine development. Vaccines (Basel) 9:622. https://doi.org/10.3390/vaccines9060622

24. Rastogi M, Sharma N, Singh SK. 2016. Flavivirus NS1: a multifaceted enigmatic viral protein. Virol J 13:131. https://doi.org/10.1186/s12985-016-0590-7

25. Pryor MJ, Wright PJ. 1994. Glycosylation mutants of dengue virus NS1 protein. J Gen Virol 75:1183–1187. https://doi.org/10.1099/0022-1317-75-5-1183

26. Hahn CS, Dalrymple JM, Strauss JH, Rice CM. 1987. Comparison of the virulent Asibi strain of yellow fever virus with the 17D vaccine strain derived from it. Proc Natl Acad Sci U S A 84:2019–2023. https://doi.org/10.1073/pnas.84.7.2019

27. Carbaugh DL, Lazear HM. 2020. Flavivirus envelope protein glycosylation: impacts on viral infection and pathogenesis. J Virol 94:e00104-20. https://doi.org/10.1128/JVI.00104-20

28. Holzmann H, Heinz FX, Mandl CW, Guirakhoo F, Kunz C. 1990. A single amino acid substitution in envelope protein E of tick-borne encephalitis virus leads to attenuation in the mouse model. J Virol 64:5156–5159. https://doi.org/10.1128/JVI.64.10.5156-5159.1990

29. Huerta V, Chinea G, Fleitas N, Sarría M, Sánchez J, Toledo P, Padrón G. 2008. Characterization of the interaction of domain III of the envelope protein of dengue virus with putative receptors from CHO cells. Virus Res 137:225–234. https://doi.org/10.1016/j.virusres.2008.07.022

30. Flamand M, Megret F, Mathieu M, Lepault J, Rey FA, Deubel V. 1999. Dengue virus type 1 nonstructural glycoprotein NS1 is secreted from mammalian cells as a soluble hexamer in a glycosylation-dependent fashion. J Virol 73:6104–6110. https://doi.org/10.1128/JVI.73.7.6104-6110.1999

31. Akey DL, Brown WC, Dutta S, Konwerski J, Jose J, Jurkiw TJ, DelProposto J, Ogata CM, Skiniotis G, Kuhn RJ, Smith JL. 2014. Flavivirus NS1 structures reveal surfaces for associations with membranes and the immune system. Science 343:881–885. https://doi.org/10.1126/science.1247749

32. Akey DL, Brown WC, Jose J, Kuhn RJ, Smith JL. 2015. Structure-guided insights on the role of NS1 in flavivirus infection. Bioessays: news and reviews in molecular, cellular and developmental biology37:489–494. https://doi.org/10.1002/bies.201400182

33. Avirutnan P, Zhang L, Punyadee N, Manuyakorn A, Puttikhunt C, Kasinrerk W, Malasit P, Atkinson JP, Diamond MS. 2007. Secreted NS1 of dengue virus attaches to the surface of cells via interactions with heparan sulfate and chondroitin sulfate E. PLoS Pathog 3:e183. https://doi.org/10.1371/journal.ppat.0030183

34. Brown WC, Akey DL, Konwerski JR, Tarrasch JT, Skiniotis G, Kuhn RJ, Smith JL. 2016. Extended surface for membrane association in Zika virus Ns1 structure. Nat Struct Mol Biol 23:865–867. https://doi.org/10.1038/nsmb.3268

35. Ci Y, Liu Z-Y, Zhang N-N, Niu Y, Yang Y, Xu C, Yang W, Qin C-F, Shi L. 2020. Zika NS1-induced ER remodeling is essential for viral replication. J Cell Biol 219:e201903062. https://doi.org/10.1083/jcb.201903062

36. Conde JN, da Silva EM, Allonso D, Coelho DR, Andrade I da S, de Medeiros LN, Menezes JL, Barbosa AS, Mohana-Borges R. 2016. Inhibition of the membrane attack complex by dengue virus NS1 through interaction with vitronectin and terminal complement proteins. J Virol 90:9570–9581. https://doi.org/10.1128/JVI.00912-16

37. Muylaert IR, Chambers TJ, Galler R, Rice CM. 1996. Mutagenesis of the N-linked glycosylation sites of the yellow fever virus NS1 protein: effects on virus replication and mouse neurovirulence. Virology 222:159–168. https://doi.org/10.1006/viro.1996.0406

38. Tamura T, Torii S, Kajiwara K, Anzai I, Fujioka Y, Noda K, Taguwa S, Morioka Y, Suzuki R, Fauzyah Y, Ono C, Ohba Y, Okada M, Fukuhara T, Matsuura Y. 2022. Secretory glycoprotein NS1 plays a crucial role in the particle formation of flaviviruses. PLoS Pathog 18:e1010593. https://doi.org/10.1371/journal.ppat.1010593

39. Youn S, Cho H, Fremont DH, Diamond MS. 2010. A short N-terminal peptide motif on flavivirus nonstructural protein NS1 modulates cellular targeting and immune recognition. J Virol 84:9516–9532. https://doi.org/10.1128/JVI.00775-10

40. Winkler G, Randolph VB, Cleaves GR, Ryan TE, Stollar V. 1988. Evidence that the mature form of the flavivirus nonstructural protein NS1 is a dimer. Virology 162:187–196. https://doi.org/10.1016/0042-6822(88)90408-4

41. Neufeldt CJ, Cortese M, Acosta EG, Bartenschlager R. 2018. Rewiring cellular networks by members of the *Flaviviridae* family. Nat Rev Microbiol 16:125–142. https://doi.org/10.1038/nrmicro.2017.170

42. Lindenbach BD, Rice CM. 1999. Genetic interaction of flavivirus nonstructural proteins NS1 and NS4A as a determinant of replicase function. J Virol 73:4611–4621. https://doi.org/10.1128/JVI.73.6.4611-4621.1999

43. Youn S, Li T, McCune BT, Edeling MA, Fremont DH, Cristea IM, Diamond MS. 2012. Evidence for a genetic and physical interaction between nonstructural proteins NS1 and NS4B that modulates replication of

West Nile virus. J Virol 86:7360–7371. https://doi.org/10.1128/JVI.00157-12

44. Avirutnan P, Fuchs A, Hauhart RE, Somnuke P, Youn S, Diamond MS, Atkinson JP. 2010. Antagonism of the complement component C4 by flavivirus nonstructural protein NS1. J Exp Med 207:793–806. https://doi.org/10.1084/jem.20092545

45. Noisakran S, Dechtawewat T, Avirutnan P, Kinoshita T, Siripanyaphinyo U, Puttikhunt C, Kasinrerk W, Malasit P, Sittisombut N. 2008. Association of dengue virus NS1 protein with lipid rafts. J Gen Virol 89:2492–2500. https://doi.org/10.1099/vir.0.83620-0

46. Pletnev AG, Bray M, Lai CJ. 1993. Chimeric tick-borne encephalitis and dengue type 4 viruses: effects of mutations on neurovirulence in mice. J Virol 67:4956–4963. https://doi.org/10.1128/JVI.67.8.4956-4963.1993

47. Whiteman MC, Li L, Wicker JA, Kinney RM, Huang C, Beasley DWC, Chung KM, Diamond MS, Solomon T, Barrett ADT. 2010. Development and characterization of non-glycosylated E and NS1 mutant viruses as a potential candidate vaccine for West Nile virus. Vaccine 28:1075–1083. https://doi.org/10.1016/j.vaccine.2009.10.112

48. Whiteman MC, Popov V, Sherman MB, Wen J, Barrett ADT. 2015. Attenuated West Nile virus mutant NS1130-132QQA/175A/207A exhibits virus-induced ultrastructural changes and accumulation of protein in the endoplasmic reticulum. J Virol 89:1474–1478. https://doi.org/10.1128/JVI.02215-14

49. Yap SSL, Nguyen-Khuong T, Rudd PM, Alonso S. 2017. Dengue virus glycosylation: what do we know? Front Microbiol 8:1415. https://doi.org/10.3389/fmicb.2017.01415

50. Putnak JR, Charles PC, Padmanabhan R, Irie K, Hoke CH, Burke DS. 1988. Functional and antigenic domains of the dengue-2 virus nonstructural glycoprotein NS-1. Virology 163:93–103. https://doi.org/10.1016/0042-6822(88)90236-x

51. Cheung AM, Yip EZ, Ashbrook AW, Goonawardane N, Quirk C, Rice CM, MacDonald MR, Hoffmann H-H. 2023. Characterization of live-attenuated Powassan virus vaccine candidates identifies an efficacious prime-boost strategy for mitigating Powassan virus disease in a murine model. Vaccines (Basel) 11:612. https://doi.org/10.3390/vaccines11030612

52. Pletnev AG, Bray M, Huggins J, Lai CJ. 1992. Construction and characterization of chimeric tick-borne encephalitis/dengue type 4 viruses. Proc Natl Acad Sci U S A 89:10532–10536. https://doi.org/10.1073/pnas.89.21.10532

53. Shan C, Xie X, Muruato AE, Rossi SL, Roundy CM, Azar SR, Yang Y, Tesh RB, Bourne N, Barrett AD, Vasilakis N, Weaver SC, Shi P-Y. 2016. An infectious cDNA clone of Zika virus to study viral virulence, mosquito transmission, and antiviral inhibitors. Cell Host Microbe 19:891–900. https://doi.org/10.1016/j.chom.2016.05.004

54. Shan C, Xie X, Shi PY. 2017. Reverse genetics of Zika virus. Methods Mol Biol 1602:47–58. https://doi.org/10.1007/978-1-4939-6964-7_4

55. Shi PY, Tilgner M, Lo MK, Kent KA, Bernard KA. 2002. Infectious cDNA clone of the epidemic West Nile virus from New York City. J Virol 76:5847–5856. https://doi.org/10.1128/jvi.76.12.5847-5856.2002

56. Aubry F, Nougairède A, Gould EA, de Lamballerie X. 2015. Flavivirus reverse genetic systems, construction techniques and applications: a historical perspective. Antiviral Res 114:67–85. https://doi.org/10.1016/j.antiviral.2014.12.007

57. Ávila-Pérez G, Nogales A, Park J-G, Vasquez DM, Dean DA, Barravecchia M, Perez DR, Almazán F, Martínez-Sobrido L. 2020. In vivo rescue of recombinant Zika virus from an infectious cDNA clone and its implications in vaccine development. Sci Rep 10:512. https://doi.org/10.1038/s41598-020-57545-2

58. Quan J, Tian J. 2009. Circular polymerase extension cloning of complex gene libraries and pathways. PLoS One 4:e6441. https://doi.org/10.1371/journal.pone.0006441

59. Quan J, Tian J. 2011. Circular polymerase extension cloning for high-throughput cloning of complex and combinatorial DNA libraries. Nat Protoc 6:242–251. https://doi.org/10.1038/nprot.2010.181

60. Setoh YX, Prow NA, Peng N, Hugo LE, Devine G, Hazlewood JE, Suhrbier A, Khromykh AA, Duprex WP, Evans J, Pierson T. 2017. De Novo generation and characterization of new Zika virus isolate using sequence data from a microcephaly case. mSphere 2:e00190-17. https://doi.org/10.1128/mSphereDirect.00190-17

61. Setoh YX, Prow NA, Rawle DJ, Tan CSE, Edmonds JH, Hall RA, Khromykh AA. 2015. Systematic analysis of viral genes responsible for differential virulence between American and Australian West Nile virus strains. J Gen Virol 96:1297–1308. https://doi.org/10.1099/vir.0.000069

62. Amarilla AA, Sng JDJ, Parry R, Deerain JM, Potter JR, Setoh YX, Rawle DJ, Le TT, Modhiran N, Wang X, Peng NYG, Torres FJ, Pyke A, Harrison JJ, Freney ME, Liang B, McMillan CLD, Cheung STM, Guevara D, Hardy JM, Bettington M, Muller DA, Coulibaly F, Moore F, Hall RA, Young PR, Mackenzie JM, Hobson-Peters J, Suhrbier A, Watterson D, Khromykh AA. 2021. A Versatile reverse genetics platform for SARS-CoV-2 and other positive-strand RNA viruses. Nat Commun 12:3431. https://doi.org/10.1038/s41467-021-23779-5

63. Edmonds J, van Grinsven E, Prow N, Bosco-Lauth A, Brault AC, Bowen RA, Hall RA, Khromykh AA. 2013. A novel bacterium-free method for generation of flavivirus infectious DNA by circular polymerase extension reaction allows accurate recapitulation of viral heterogeneity. J Virol 87:2367–2372. https://doi.org/10.1128/JVI.03162-12

64. Tamura Tet al. 2019. In vivo dynamics of reporter Flaviviridae viruses. J Virol 93:22.

65. Torii S, Ono C, Suzuki R, Morioka Y, Anzai I, Fauzyah Y, Maeda Y, Kamitani W, Fukuhara T, Matsuura Y. 2021. Establishment of a reverse genetics system for SARS-CoV-2 using circular polymerase extension reaction. Cell Rep 35:109014. https://doi.org/10.1016/j.celrep.2021.109014

66. Sanchez-Velazquez R, de Lorenzo G, Tandavanitj R, Setthapramote C, Bredenbeek PJ, Bozzacco L, MacDonald MR, Clark JJ, Rice CM, Patel AH, Kohl A, Varjak M. 2020. Generation of a reporter yellow fever virus for high throughput antiviral assays. Antiviral Res 183:104939. https://doi.org/10.1016/j.antiviral.2020.104939

67. Tamura T, Zhang J, Madan V, Biswas A, Schwoerer MP, Cafiero TR, Heller BL, Wang W, Ploss A. 2022. Generation and characterization of genetically and antigenically diverse infectious clones of dengue virus serotypes 1-4. Emerg Microbes Infect 11:227–239. https://doi.org/10.1080/22221751.2021.2021808

68. Hobson-Peters J, Harrison JJ, Watterson D, Hazlewood JE, Vet LJ, Newton ND, Warrilow D, Colmant AMG, Taylor C, Huang B, Piyasena TBH, Chow WK, Setoh YX, Tang B, Nakayama E, Yan K, Amarilla AA, Wheatley S, Moore PR, Finger M, Kurucz N, Modhiran N, Young PR, Khromykh AA, Bielefeldt-Ohmann H, Suhrbier A, Hall RA. 2019. A recombinant platform for flavivirus vaccines and diagnostics using chimeras of a new insect-specific virus. Sci Transl Med 11:eaax7888. https://doi.org/10.1126/scitranslmed.aax7888

69. Hyun S-I, Maruri-Avidal L, Moss B. 2015. Topology of endoplasmic reticulum-associated cellular and viral proteins determined with split-GFP. Traffic 16:787–795. https://doi.org/10.1111/tra.12281

70. Kaddoum L, Magdeleine E, Waldo GS, Joly E, Cabantous S. 2010. One-step split GFP staining for sensitive protein detection and localization in mammalian cells. Biotechniques 49:727–728. https://doi.org/10.2144/000113512

71. Kamiyama D, Sekine S, Barsi-Rhyne B, Hu J, Chen B, Gilbert LA, Ishikawa H, Leonetti MD, Marshall WF, Weissman JS, Huang B. 2016. Versatile protein tagging in cells with split fluorescent protein. Nat Commun 7:11046. https://doi.org/10.1038/ncomms11046

72. Romei MG, Boxer SG. 2019. Split green fluorescent proteins: scope, limitations, and outlook. Annu Rev Biophys 48:19–44. https://doi.org/10.1146/annurev-biophys-051013-022846

73. Sasaki M, Anindita PD, Phongphaew W, Carr M, Kobayashi S, Orba Y, Sawa H. 2018. Development of a rapid and quantitative method for the analysis of viral entry and release using a NanoLuc luciferase complementation assay. Virus Res 243:69–74. https://doi.org/10.1016/j.virusres.2017.10.015

74. Avilov SV, Moisy D, Munier S, Schraidt O, Naffakh N, Cusack S. 2012. Replication-competent influenza A virus that encodes a split-green fluorescent protein-tagged PB2 polymerase subunit allows live-cell imaging of the virus life cycle. J Virol 86:1433–1448. https://doi.org/10.1128/JVI.05820-11

75. Fan H, Qiao L, Kang K-D, Fan J, Wei W, Luo G, Ou J-H. 2017. Attachment and postattachment receptors important for hepatitis C virus infection and cell-to-cell transmission. J Virol 91:13. https://doi.org/10.1128/JVI.00280-17

76. Brimacombe CL, Grove J, Meredith LW, Hu K, Syder AJ, Flores MV, Timpe JM, Krieger SE, Baumert TF, Tellinghuisen TL, Wong-Staal F, Balfe P,

McKeating JA. 2011. Neutralizing antibody-resistant hepatitis C virus cell-to-cell transmission. J Virol 85:596–605. https://doi.org/10.1128/JVI.01592-10

77. Timpe JM, Stamataki Z, Jennings A, Hu K, Farquhar MJ, Harris HJ, Schwarz A, Desombere I, Roels GL, Balfe P, McKeating JA. 2008. Hepatitis C virus cell-cell transmission in hepatoma cells in the presence of neutralizing antibodies. Hepatology 47:17–24. https://doi.org/10.1002/hep.21959

78. Cifuentes-Munoz N, El Najjar F, Dutch RE. 2020. Viral cell-to-cell spread: conventional and non-conventional ways. Adv Virus Res 108:85–125. https://doi.org/10.1016/bs.aivir.2020.09.002

79. Conde JN, Schutt WR, Mladinich M, Sohn S-Y, Hearing P, Mackow ER. 2020. NS5 sumoylation directs nuclear responses that permit Zika virus to persistently infect human brain microvascular endothelial cells. J Virol 94:e01086-20. https://doi.org/10.1128/JVI.01086-20

80. Mladinich MC, Conde JN, Schutt WR, Sohn S-Y, Mackow ER. 2021. Blockade of autocrine CCL5 responses inhibits Zika virus persistence and spread in human brain microvascular endothelial cells. mBio 12:e0196221. https://doi.org/10.1128/mBio.01962-21

81. Mason PW. 1989. Maturation of Japanese encephalitis virus glycoproteins produced by infected mammalian and mosquito cells. Virology 169:354–364. https://doi.org/10.1016/0042-6822(89)90161-x

82. Mason PW, McAda PC, Mason TL, Fournier MJ. 1987. Sequence of the dengue-1 virus genome in the region encoding the three structural proteins and the major nonstructural protein NS1. Virology 161:262–267. https://doi.org/10.1016/0042-6822(87)90196-6

83. Mandl CW, Heinz FX, Stöckl E, Kunz C. 1989. Genome sequence of tick-borne encephalitis virus (western subtype) and comparative analysis of nonstructural proteins with other flaviviruses. Virology 173:291–301. https://doi.org/10.1016/0042-6822(89)90246-8

84. Mirdita M, Schütze K, Moriwaki Y, Heo L, Ovchinnikov S, Steinegger M. 2022. Colabfold: making protein folding accessible to all. Nat Methods 19:679–682. https://doi.org/10.1038/s41592-022-01488-1

85. Leonetti MD, Sekine S, Kamiyama D, Weissman JS, Huang B. 2016. A scalable strategy for high-throughput GFP tagging of endogenous human proteins. Proc Natl Acad Sci U S A 113:E3501–3508. https://doi.org/10.1073/pnas.1606731113

86. Schoggins JW, Dorner M, Feulner M, Imanaka N, Murphy MY, Ploss A, Rice CM. 2012. Dengue reporter viruses reveal viral dynamics in interferon receptor-deficient mice and sensitivity to interferon effectors in vitro. Proc Natl Acad Sci U S A 109:14610–14615. https://doi.org/10.1073/pnas.1212379109

87. Singh BK, Hornick AL, Krishnamurthy S, Locke AC, Mendoza CA, Mateo M, Miller-Hunt CL, Cattaneo R, Sinn PL, Lyles DS. 2015. The Nectin-4/Afadin protein complex and intercellular membrane pores contribute to rapid spread of measles virus in primary human airway epithelia. J Virol 89:7089–7096. https://doi.org/10.1128/JVI.00821-15

88. Lauer AN, Tenenbaum T, Schroten H, Schwerk C. 2018. The diverse cellular responses of the choroid plexus during infection of the central nervous system. Am J Physiol Cell Physiol 314:C152–C165. https://doi.org/10.1152/ajpcell.00137.2017

89. Schwerk C, Tenenbaum T, Kim KS, Schroten H. 2015. The choroid plexus-a multi-role player during infectious diseases of the CNS. Front Cell Neurosci 9:80. https://doi.org/10.3389/fncel.2015.00080

90. Thompson D, Brissette CA, Watt JA. 2022. The choroid plexus and its role in the pathogenesis of neurological infections. Fluids Barriers CNS 19:75. https://doi.org/10.1186/s12987-022-00372-6

91. Carbaugh DL, Baric RS, Lazear HM. 2019. Envelope protein glycosylation mediates Zika virus pathogenesis. J Virol 93:12. https://doi.org/10.1128/JVI.00113-19

92. de Wispelaere M, Yang PL. 2012. Mutagenesis of the DI/DIII Linker in dengue virus envelope protein impairs viral particle assembly. J Virol 86:7072–7083. https://doi.org/10.1128/JVI.00224-12

93. Engel AR, Rumyantsev AA, Maximova OA, Speicher JM, Heiss B, Murphy BR, Pletnev AG. 2010. The neurovirulence and neuroinvasiveness of chimeric tick-borne encephalitis/dengue virus can be attenuated by introducing defined mutations into the envelope and NS5 protein genes and the 3' non-coding region of the genome. Virology 405:243–252. https://doi.org/10.1016/j.virol.2010.06.014

94. Monath TP, Arroyo J, Levenbook I, Zhang Z-X, Catalan J, Draper K, Guirakhoo F. 2002. Single mutation in the flavivirus envelope protein hinge region increases neurovirulence for mice and monkeys but decreases viscerotropism for monkeys: relevance to development and safety testing of live, attenuated vaccines. J Virol 76:1932–1943. https://doi.org/10.1128/jvi.76.4.1932-1943.2002

95. Whiteman MC, Wicker JA, Kinney RM, Huang C-H, Solomon T, Barrett ADT. 2011. Multiple amino acid changes at the first lycosylation motif in NS1 protein of West Nile virus are necessary for complete attenuation for mouse neuroinvasiveness. Vaccine 29:9702–9710. https://doi.org/10.1016/j.vaccine.2011.09.036

96. Fishburn AT, Pham OH, Kenaston MW, Beesabathuni NS, Shah PS. 2022. Let's get physical: flavivirus-host protein-protein interactions in replication and pathogenesis. Front Microbiol 13:847588.

97. Baker C, Shi PY. 2020. Construction of stable reporter flaviviruses and their applications. Viruses 12:1082. https://doi.org/10.3390/v12101082

98. Kienzle C, von Blume J. 2014. Secretory cargo sorting at the trans-golgi network. Trends Cell Biol 24:584–593. https://doi.org/10.1016/j.tcb.2014.04.007

99. Sager G, Gabaglio S, Sztul E, Belov GA. 2018. Role of host cell secretory machinery in Zika virus life cycle. Viruses 10:559. https://doi.org/10.3390/v10100559

100. Longo PA, Kavran JM, Kim M-S, Leahy DJ. 2013. Transient mammalian cell transfection with polyethylenimine (PEI). Methods Enzymol 529:227–240. https://doi.org/10.1016/B978-0-12-418687-3.00018-5

101. Lyskov S, Chou F-C, Conchúir SÓ, Der BS, Drew K, Kuroda D, Xu J, Weitzner BD, Renfrew PD, Sripakdeevong P, Borgo B, Havranek JJ, Kuhlman B, Kortemme T, Bonneau R, Gray JJ, Das R, Uversky VN. 2013. Serverification of molecular modeling applications: the Rosetta online server that includes everyone (ROSIE). PLoS ONE 8:e63906. https://doi.org/10.1371/journal.pone.0063906

102. Moretti R, Lyskov S, Das R, Meiler J, Gray JJ. 2018. Web-accessible molecular modeling with Rosetta: the Rosetta online server that includes everyone (ROSIE). Protein Sci 27:259–268. https://doi.org/10.1002/pro.3313